

# Citrate-Induced Aggregation of Conjugated Polyelectrolytes for Al<sup>3+</sup>-Ion-Sensing Assays

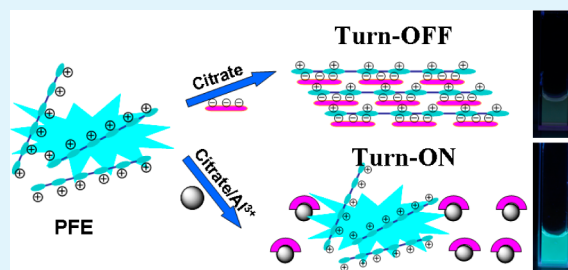
Hui Wang, Fang He,\* Rongjian Yan, Xiaoyu Wang, Xi Zhu, and Lidong Li\*

School of Materials Science and Engineering, University of Science and Technology Beijing, Beijing 100083, People's Republic of China

## Supporting Information

**ABSTRACT:** This work shows the sodium citrate induced efficient interpolymer  $\pi$ -stacking aggregation of the planar cationic conjugated polyelectrolyte poly[{9,9-bis[6'-(*N,N*-trimethylamino)hexyl]-2,7-fluorenyleneethynylene}-*alt-co*-(1,4-phenylene)] dibromide (PFE) in aqueous solution, which results in the self-quenching of fluorescence. Using the citrate-induced aggregation properties of PFE and the strong chelation ability of citrate with aluminum ions (Al<sup>3+</sup>), a sensitive and selective Al<sup>3+</sup>-ion detection assay in aqueous solution was developed through monitoring of the fluorescence recovery of PFE. The fluorescence intensity recovery of PFE depends on the concentration of Al<sup>3+</sup> ions, and linear fluorescence recovery was observed in the range of 0.5–9  $\mu$ M. The limit of detection of this assay is 0.37  $\mu$ M. Its simplicity and rapidity mean this assay shows promise for the real-time detection of Al<sup>3+</sup>.

**KEYWORDS:** conjugated polymer, fluorescence, aggregation, citrate, chelation, ion detection



## INTRODUCTION

Conjugated polyelectrolytes (CPEs) have a unique  $\pi$ -conjugated backbone. The excitation energy transferring along the backbone of CPEs to the energy/electron acceptor can result in the amplification of fluorescent signals.<sup>1</sup> Therefore, sensitive and selective metal ions such as Hg<sup>2+</sup>, Ag<sup>+</sup>, Pb<sup>2+</sup>, Cu<sup>2+</sup>, and Fe<sup>3+</sup> sensors based on CPEs have been developed through the modification of metal binding units such as nitrogen ligands, ionic groups, and crown ether groups on the polyelectrolyte side chains or on the polymer backbones,<sup>1–11</sup> However, to the best of our knowledge, until now only one selective Al<sup>3+</sup> sensor system using complicated CPE nanoparticles has been reported.<sup>11</sup>

An inorganic aluminum ion is considered toxic in many biological processes. Excessive ingestion of these inorganic Al<sup>3+</sup> ions to the human body can lead to many diseases such as osteoporosis, dementia, myopathy, and Alzheimer's disease.<sup>12,13</sup> Moreover, the excessive exposure of living plants to Al<sup>3+</sup> also can limit the growth of plants.<sup>14,15</sup> While acidic rain and human activities can increase the concentration of Al<sup>3+</sup> in soils, human foods, and drink water, the development of sensitive and selective detection sensors of Al<sup>3+</sup> for water and food quality assessment is highly important for human health and the environment. In this regard, some fluorescent sensors based on small organic dyes have been developed.<sup>16–25</sup> However, until now, majority of these sensors show moderate sensitivity and selectivity to Al<sup>3+</sup>. And only a few of them can detect the Al<sup>3+</sup> in absolute aqueous solution, which limited their practical application.

CPEs have attracted much attention for developing sensitive chem- and biosensors. However, most of the sensors are based

on the fluorescence intensity change of CPEs induced by electron transfer or energy transfer between the CPEs and binding analytes. Specifically, some kinds of CPEs such as poly(*p*-phenyleneethynylene) (PPE), poly(*p*-phenylenevinylene) (PPV), polythiophene, and polyfluorene derivatives have been developed as sensors based on the fluorescence self-quenching properties resulting from their analyte-induced tight aggregation with high charge density.<sup>26–34</sup> Using this unique property, CPEs can be applied in the detection of biomacromolecules such as protein,<sup>26–29</sup> DNA,<sup>30</sup> and heparin.<sup>31</sup> However, until now, only a few works were reported about small-molecule analytes inducing the aggregation-sensitive fluorescence properties of CPEs.<sup>32–34</sup>

In this paper, we investigate the aggregation-induced photophysical properties of the CPE poly[{9,9-bis[6'-(*N,N*-trimethylamino)hexyl]-2,7-fluorenyleneethynylene}-*alt-co*-(1,4-phenylene)] dibromide, which contains fluorene units in the PPE-like structure. We found that the small molecular sodium citrate can induce tight aggregation and then result in amplified fluorescence self-quenching of PFE. Al<sup>3+</sup> ions can selectively chelate with sodium citrate. Therefore, using the citrate-induced aggregation properties of PFE, we developed an efficient and simple assay to detect Al<sup>3+</sup> in aqueous solution.

## EXPERIMENTAL SECTION

**Materials and Measurements.** Conjugated polymers poly[{9,9-bis[6'-(*N,N*-trimethylamino)hexyl]-2,7-fluorenyleneethynylene}-*alt*

Received: June 24, 2013

Accepted: July 23, 2013

Published: July 23, 2013

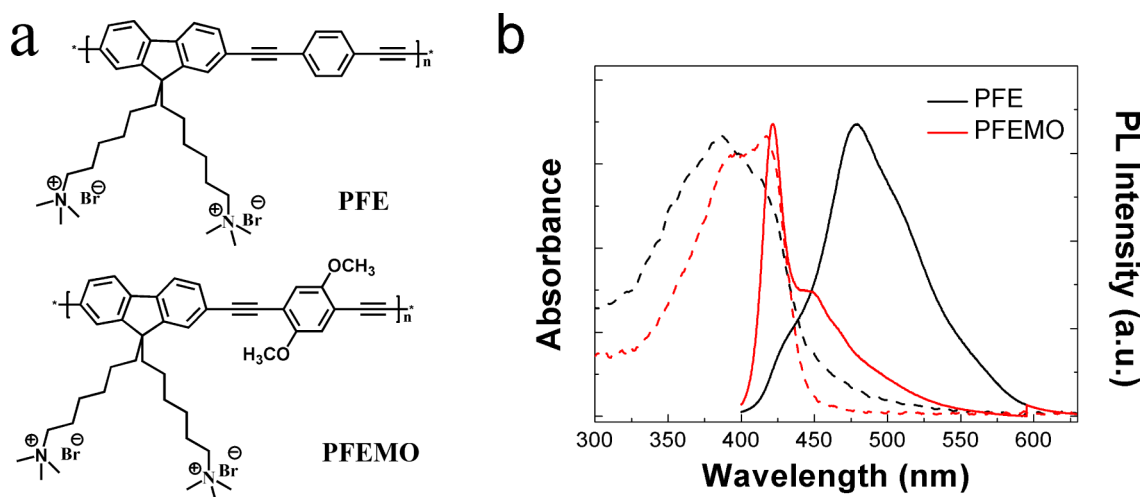


**Figure 1.** (a) Chemical structures of polymers PFE and PFEMO. (b) Normalized absorption and emission spectra of PFE and PFEMO in H<sub>2</sub>O.

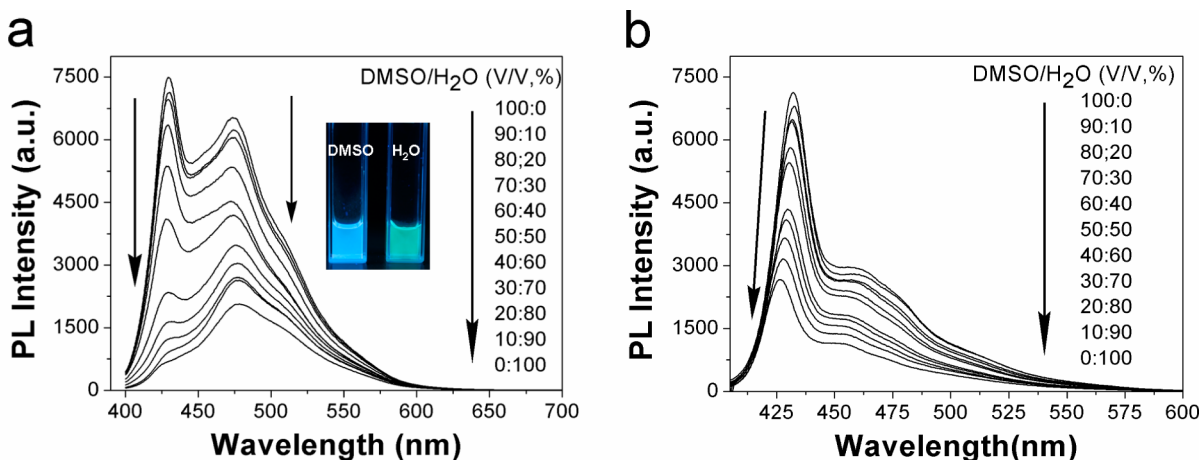


**Figure 2.** (a) Emission spectra of PFE and (b) PFEMO in DMSO/H<sub>2</sub>O with different volume ratios (shown as percentages). [PFE] =  $2.5 \times 10^{-6}$  M, and [PFEMO] =  $2.5 \times 10^{-7}$  M. The excited wavelength is 383 nm.

co-(1,4-phenylene)] dibromide (PFE)<sup>35</sup> and poly[9,9-bis[6'-(*N,N*-trimethylamino)hexyl]-2,7-fluorenyleneethynylene]-*alt-co*-1,4-(2,5-dimethoxy)phenylene] dibromide (PFEMO)<sup>36</sup> were synthesized according to our previous procedures reported in the literature. The organic acid salts were purchased from J&K Chemical Co. Al(NO<sub>3</sub>)<sub>3</sub>, MnCl<sub>2</sub>, MgSO<sub>4</sub>, FeCl<sub>2</sub>, FeCl<sub>3</sub>, CuCl<sub>2</sub>, CoCl<sub>2</sub>, CrCl<sub>3</sub>, Hg(ClO<sub>4</sub>)<sub>2</sub>, AgNO<sub>3</sub>, Pb(NO<sub>3</sub>)<sub>2</sub>, ZnCl<sub>2</sub>, and GaCl<sub>3</sub> were obtained from Alfa Aesar. Other chemicals were purchased from Beijing Chemical Co. All reagents were used as received without further purification. UV-vis absorption and fluorescence emission spectra were measured on a Hitachi U-3900H spectrophotometer and a Hitachi F-7000 fluorescence spectrophotometer, respectively. Ultrapure Millipore water (18.3 MΩ·cm) was used in experiments.

**Citrate-Induced Aggregation of PFE.** To a solution of PFE [1 mL, [PFE] =  $1.0 \times 10^{-5}$  M in repeat units (RUs)] in water and a solution of PFE (1 mL, [PFE] =  $2.5 \times 10^{-6}$  M in RUs) in dimethyl sulfoxide (DMSO) were respectively and successively added 0–60 μL amounts of sodium citrate ([sodium citrate] =  $1.0 \times 10^{-4}$  M) at room temperature. Fluorescence spectra were measured at an excitation wavelength at 383 nm. The assay procedures for sodium benzoate, sodium lactate, sodium oxalate, sodium malate, sodium tartrate, sodium succinate, and ethylenediaminetetraacetic acid tetrasodium salt (tetrasodium EDTA) were the same as that for sodium citrate. Moreover, to a solution of PFE (2 mL, [PFE] =  $5.0 \times 10^{-5}$  M in RUs) in water were respectively added 0–60 μL amounts of sodium citrate ([sodium citrate] =  $1.0 \times 10^{-3}$  M) at room temperature. UV-vis absorption spectra were measured in the range of 300–600 nm.

**Al<sup>3+</sup> Detection.** To aqueous solutions of sodium citrate (1 mL, [sodium citrate] =  $6.0 \times 10^{-6}$  M) were respectively added 0, 0.5, 1, 1.5, 2, 3, 4, 6, 9, 10, 12, 16, and 20 μL of Al<sup>3+</sup> ([Al<sup>3+</sup>] =  $1 \times 10^{-3}$  M) at room temperature. Solutions were mixed thoroughly to form Al<sup>3+</sup>/citrate complexes. Then, 10 μL of PFE ([PFE] =  $1.0 \times 10^{-3}$  M in RUs) was added to each solution. Fluorescence spectra were measured with an excitation wavelength at 383 nm. The assay procedures for the other metal ions were the same as that for Al<sup>3+</sup>.

For the influence of isolated metal ions on the emission of PFE, 10 μL of each metal ion ([metal ion] =  $1 \times 10^{-3}$  M) was added to 1 mL of PFE ([PFE] =  $1.0 \times 10^{-5}$  M in RUs) in H<sub>2</sub>O. Fluorescence spectra were measured with an excitation wavelength at 383 nm.

For Al<sup>3+</sup> detection in solution with different pH values, 10 μL of PFE ([PFE] =  $1.0 \times 10^{-3}$  M in RUs) was respectively added to 1 mL of a phosphate buffer solution (PBS; 10 mM) with different pH values (3.0, 5.0, 7.0, 8.0, 9.0, and 11.0). Then, 60 μL of sodium citrate ([sodium citrate] =  $1.0 \times 10^{-4}$  M) was added to each solution, and fluorescence spectra were measured with an excitation wavelength at 383 nm. To a PBS solution (10 mM) of sodium citrate (1 mL, [sodium citrate] =  $6.0 \times 10^{-6}$  M) at different pH values (3.0, 5.0, 7.0, 8.0, 9.0, and 11.0) was added 9 μL of Al<sup>3+</sup> ([Al<sup>3+</sup>] =  $1 \times 10^{-3}$  M) at room temperature. Then, 10 μL of PFE ([PFE] =  $1.0 \times 10^{-3}$  M in RUs) was added to each solution after these solutions were mixed thoroughly. Fluorescence spectra were measured with an excitation wavelength at 383 nm.

## RESULTS AND DISCUSSION

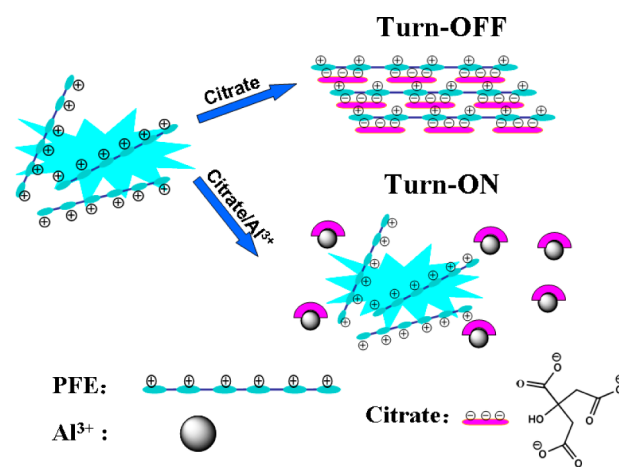
PFE with cationic side groups was selected in our assay for their unique optical properties. The chemical structure of PFE is shown in Figure 1a. First, the UV–vis absorption and fluorescence spectra of PFE in H<sub>2</sub>O were investigated. As shown in Figure 1b, PFE exhibited an absorption peak at around 386 nm and a broad emission peak at around 479 nm. To further understand the optical properties of PFE, we also synthesized PFEMO, which has a structure similar to that of PFE except that the *p*-phenylene units were substituted by 1,4-(2,5-dimethoxy)phenylene ones. The absorption spectra of PFEMO exhibited a slightly red-shifted peak at 394 nm with a higher shoulder at 416 nm, for the contribution of the nonbonding electron pairs on the oxygen atoms to conjugation of the polymer chains.<sup>37,38</sup> However, the emission spectrum of PFEMO in Figure 1b exhibited a peak at 421 nm, with a vibronic shoulder at 448 nm in H<sub>2</sub>O. The emission peak of PFEMO was blue shifted by about 58 nm compared with that of PFE in H<sub>2</sub>O.

Then, to investigate the red-shift emission of PFE in H<sub>2</sub>O, we studied the absorption and emission properties of PFE and PFEMO in a mixed solution with different volume ratios of DMSO to H<sub>2</sub>O. DMSO is a good solvent for PFE and PFEMO and can reduce the aggregation of the polymers in the solution. As the proportion of H<sub>2</sub>O was increased, the absorption spectra of PFE showed no obvious change (Figure S1 in the Supporting Information). However, as shown in Figure 2a, PFE exhibited maximum emission at 430 nm with a shoulder at 474 nm in pure DMSO. Upon addition of H<sub>2</sub>O, the emission at 430 nm gradually decreased in intensity. The emission at 430 nm almost disappeared, and the peak at 474 nm was slightly red-shifted to 479 nm in pure H<sub>2</sub>O. The color of the solution also changed from blue to green after excitation with a 365 nm UV lamp (inset of Figure 2a). Emission spectra of PFEMO in DMSO/H<sub>2</sub>O mixtures with different volume ratios revealed that the gradual addition of H<sub>2</sub>O to DMSO caused the fluorescence intensity to decrease with a slight blue shift (10 nm) of the emission maximum. However, the shape of the emission spectra changed little (Figure 2b).

From the experience of PPE derivatives, it is known to show red shifts of their emission spectra for two reasons. One is  $\pi$ – $\pi$  stacking of the polymer chains to form interchain cofacial aggregation.<sup>39</sup> The resulting loss of vibrational structure induces red-shifted excimer-type emission. The other is aggregation-induced planarization of the conjugated backbone, in which the vibrational structure of the polymer backbone is preserved. The absorption and emission spectra of PFE and PFEMO did not exhibit new peaks in different solvents. Therefore, we propose that the aggregation of PFE in H<sub>2</sub>O was induced by planarization of the backbone and not  $\pi$ – $\pi$  stacking cofacial aggregation. A comparison of the optical properties of PFE and PFEMO in DMSO and aqueous solutions demonstrated that PFE has more rigid polymer chains that can be planarized more easily than PFEMO. The methoxy groups of PFEMO decreased the planarization ability of polymer chains.<sup>39</sup> PFE mainly displayed aggregation-induced backbone planarization in aqueous solution. It may have a stable response to analytes in aqueous solution.

Then, the mechanism of our Al<sup>3+</sup> ion sensor based on PFE is illustrated in Scheme 1. The assay was designed based on the ability of Al<sup>3+</sup> ions to chelate more strongly with citrate than other metal ions.<sup>40</sup> Citrate can induce interpolymer aggregation

Scheme 1. Schematic Representation of the Al<sup>3+</sup> Assay



and result in fluorescence self-quenching of PFE in water. In the absence of Al<sup>3+</sup> ions, the fluorescence of PFE was “turned off” by citrate. However, upon the addition of Al<sup>3+</sup> ions to the solution containing citrate, the formation of citrate/Al<sup>3+</sup> complexes induced the separation of the polymer chains, causing PFE to exhibit strong fluorescence.

First, we investigated the fluorescence response of PFE to oppositely charged sodium citrate. As shown in Figure 3a, upon the addition of sodium citrate ( $0\text{--}6 \times 10^{-6}$  M) to a solution of PFE ( $1 \times 10^{-5}$  M) in H<sub>2</sub>O, the emission intensity of PFE was quenched. Up to 83% quenching was observed when 6  $\mu$ M sodium citrate was added. From the linear Stern–Volmer plot in low concentrations of sodium citrate, the quenching efficiency of the citrate was determined with a Stern–Volmer constant ( $K_{SV}$ ) value of  $2.66 \times 10^5$  M<sup>-1</sup>. To study the mechanism of fluorescence quenching, we examined the interaction of seven other organic acid salts with PFE under the same conditions (Figure S2 in the Supporting Information). Seven organic acid salts with different anionic charge densities were used: tetrasodium EDTA, sodium tartrate, sodium succinate, sodium benzoate, sodium lactate, sodium oxalate, and sodium malate. As shown in Figure 3b, less than a 15% decrease in the emission intensity of PFE at 479 nm was observed for the mono- and diacid salts. The  $K_{SV}$  values for these mono- and diacid salts were around  $2.0 \times 10^4$  M<sup>-1</sup>, which is about 13 times lower than that of citrate. For tetrasodium EDTA with four negative charges per molecule, up to 62% quenching was also observed. The quenching efficiency is smaller than that of sodium citrate. Moreover, the UV–vis absorption spectra of PFE in the presence of different concentrations of citrate showed that the addition of citrate only reduced the absorbance of PFE; no obvious shift of the absorption peak was observed (Figure S3 in the Supporting Information). Therefore, we propose that PFE can selectively form interpolymer  $\pi$ -stacking aggregation with sodium citrate through relatively strong electrostatic interactions, which results in efficient fluorescence self-quenching of PFE.

Interestingly, when sodium citrate ( $0\text{--}6 \times 10^{-6}$  M) was added to a solution of less PFE ( $2.5 \times 10^{-6}$  M) in DMSO, the emission intensity of PFE was almost unchanged (Figure 4). Moreover, the selectivity of PFE for sodium citrate is also higher than that of PFEMO, as determined from a quenching efficiency plot of PFEMO against different concentrations of organic acid salts (Figure S4 in the Supporting Information). This result illustrates that the aggregation-induced planarization

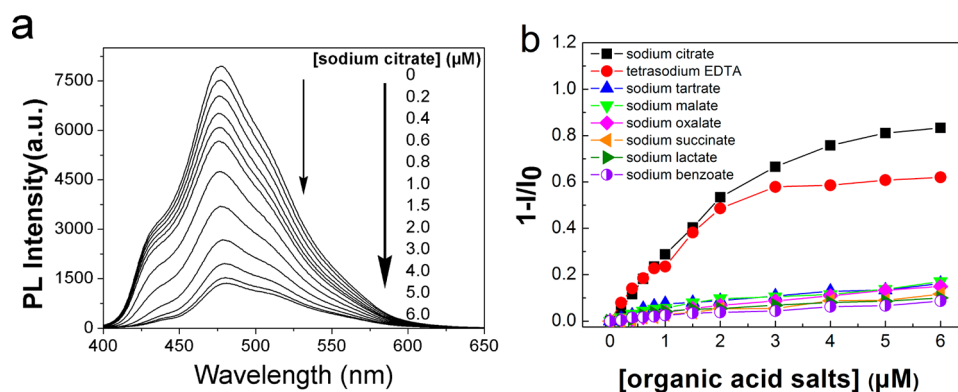


**Figure 3.** (a) Emission spectra of PFE in the presence of different concentrations of sodium citrate. (b) Quenching efficiency of PFE as a function of the concentrations of different organic acid salts. [PFE] =  $1.0 \times 10^{-5}$  M, and [sodium citrate], [tetrasodium EDTA], [sodium tartrate], [sodium malate], [sodium oxalate], [sodium succinate], [sodium lactate], and [sodium benzoate] =  $0-6.0 \times 10^{-6}$  M.

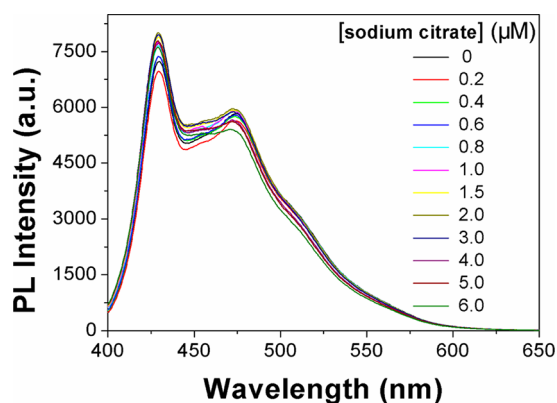


**Figure 4.** Fluorescence emission spectra of PFE in DMSO with successive additions of sodium citrate. [PFE] =  $2.5 \times 10^{-6}$  M, and [sodium citrate] =  $0-6.0 \times 10^{-6}$  M.

of the PFE chains in  $H_2O$  increased their fluorescent response to interpolymer aggregation. As a result, a sensitive response was obtained.

To confirm the ability of sodium citrate and  $Al^{3+}$  ions to chelate in this system, the emission spectra of PFE/sodium citrate complexes were measured in the absence and presence of  $Al^{3+}$  ions. As shown in Figure 5a, the addition of sodium citrate ( $6 \times 10^{-6}$  M) alone leads to marked quenching of the

emission from PFE ( $1.0 \times 10^{-5}$  M). When sodium citrate was mixed with  $Al^{3+}$  ions ( $2.0 \times 10^{-5}$  M), the emission intensity hardly changed compared with that of PFE. The control experiment illustrates that  $Al^{3+}$  ions have no effect on the fluorescence of PFE. Overall, these results demonstrate that sodium citrate and  $Al^{3+}$  ions formed stable complexes in the aqueous solution and that the sodium citrate/ $Al^{3+}$  complex with less negative charges than sodium citrate limited the interpolymer  $\pi$ -stacking aggregation of PFE.

The dependence of emission spectra of PFE ( $1.0 \times 10^{-5}$  M) as a function of the concentration of  $Al^{3+}$  ions in the presence of sodium citrate ( $6.0 \times 10^{-6}$  M) showed that the fluorescence intensity recovery of PFE depends on the concentration of  $Al^{3+}$  ions (Figure S5a,b in the Supporting Information). Nearly linear fluorescence recovery was observed in the range of  $0.5-9 \mu M$  (Figure 5b). The fluorescence intensity of PFE was almost totally recovered when the concentration of  $Al^{3+}$  ions was increased up to  $9 \mu M$ . The limit of detection (LOD) of this assay is  $0.37 \mu M$  in this condition obtained from eq 1 by five independent measurements.<sup>41</sup> In eq 1,  $S_0$  represents the standard deviation of the background and  $S$  represents the sensitivity of this assay.

$$LOD = 3 \times \frac{S_0}{S} \quad (1)$$

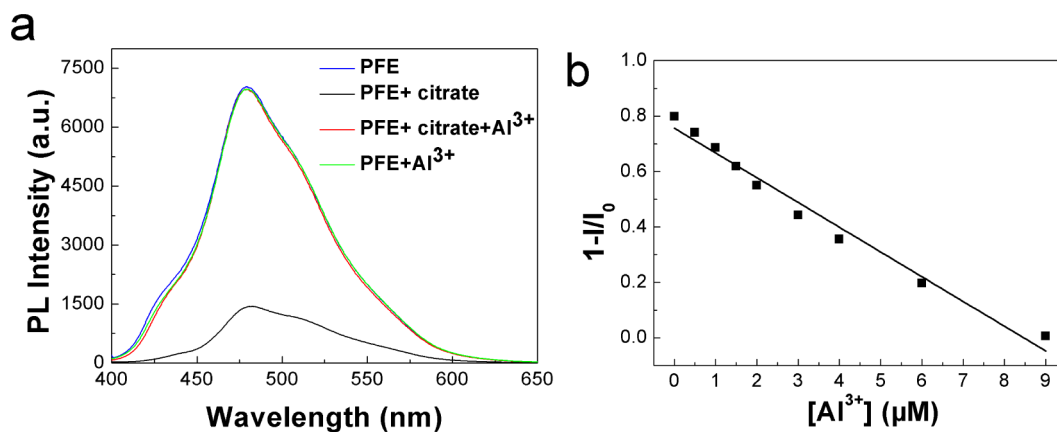


**Figure 5.** (a) Emission spectra of PFE, PFE/sodium citrate, PFE/sodium citrate/ $Al^{3+}$ , and PFE/ $Al^{3+}$  mixtures in  $H_2O$ . [ $Al^{3+}$ ] =  $2.0 \times 10^{-5}$  M. (b) Linearity of the fluorescence quenching efficiency of the PFE/sodium citrate complex as a function of the concentration of  $Al^{3+}$ . [ $Al^{3+}$ ] =  $0.5-9 \mu M$ , [PFE] =  $1.0 \times 10^{-5}$  M, and [sodium citrate] =  $6.0 \times 10^{-6}$  M.

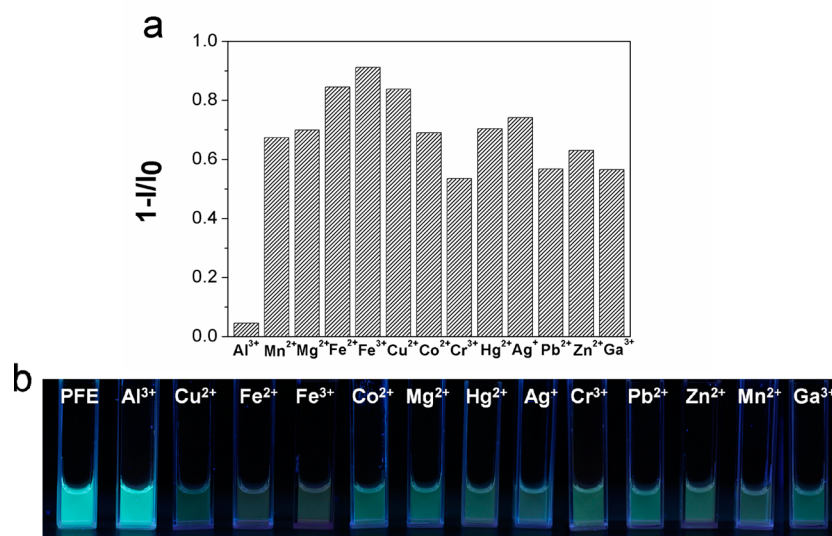


**Figure 6.** (a) Quenching efficiency of PFE/sodium citrate in the presence of various metal ions in H<sub>2</sub>O. [metal ions] =  $9.0 \times 10^{-6}$  M. (b) Fluorescence images of PFE and a PFE/sodium citrate solution under a 365 nm UV lamp in the presence of various metal ions in H<sub>2</sub>O. [metal ions] =  $9.0 \times 10^{-6}$  M, [PFE] =  $1.0 \times 10^{-5}$  M, and [sodium citrate] =  $6.0 \times 10^{-6}$  M.

Comparing the concentration of sodium citrate and Al<sup>3+</sup> in the plateau state allowed us to propose that the complex [Al<sub>3</sub>(C<sub>6</sub>H<sub>4</sub>O<sub>7</sub>)<sub>2</sub>(OH)<sub>2</sub>(H<sub>2</sub>O)<sub>4</sub>]<sup>-</sup> was formed under these conditions, consistent with a reported structure.<sup>42</sup> Moreover, we think that this assay can linearly determine the concentration of Al<sup>3+</sup> ions with a wider range by tuning the concentration of the PFE/sodium citrate complex.

Many metal ions can normally interact with citrate, which may interfere with the detection of Al<sup>3+</sup>. To examine the selectivity of this assay, the fluorescence recovery of PFE with various metal ions was investigated under identical conditions. Figure 6a shows the fluorescence quenching efficiencies of PFE in the presence of 9 μM Mn<sup>2+</sup>, Mg<sup>2+</sup>, Fe<sup>2+</sup>, Fe<sup>3+</sup>, Cu<sup>2+</sup>, Co<sup>2+</sup>, Cr<sup>3+</sup>, Hg<sup>2+</sup>, Ag<sup>+</sup>, Pb<sup>2+</sup>, Zn<sup>2+</sup>, and Ga<sup>3+</sup> ions. The results illustrated that the fluorescence of PFE was quenched by sodium citrate in the presence of these metal ions; only Cr<sup>3+</sup>, Ga<sup>3+</sup>, and Pb<sup>2+</sup> ions had little effect on the fluorescence recovery of PFE because of their weak interaction with citrate. The control experiments demonstrated that all of the metal ions alone have almost no effect on the fluorescence recovery of PFE (Figure S6 in the Supporting Information). Therefore, this platform has high sensitivity and minor interference from other metal ions.

For the further practical application of this assay, we also examine the working pH range for Al<sup>3+</sup> detection using this PFE/citrate complex. The effect of medium pH values on the quenching efficiency of PFE by citrate and on the fluorescence recovery efficiency (%) of PFE/citrate by Al<sup>3+</sup> ions were studied. As shown in Figure 7, the quenching efficiency of PFE by citrate only decreased about 30% at pH 3.0 and 11.0 for deprotonation of citrate in a strong acidic solution (pH 3.0) and PFE in a strong basic solution (pH 11.0), resulting in relatively weak electrostatic interaction. Moreover, the fluorescence of PFE can be recovered by about 95% in the acid solution (pH from 3.0 to 5.0). In the neutral and basic solutions (pH 7.0–11.0), the recovery efficiency also reached up to 70%. The results demonstrated that this assay has a wide working pH range.

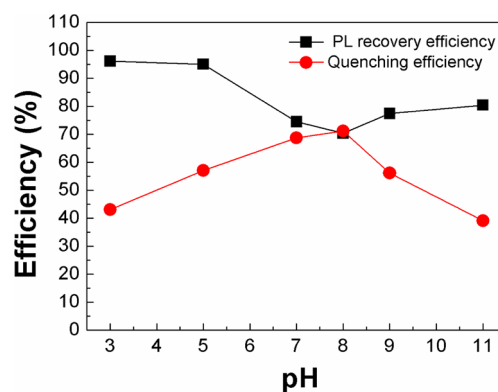


**Figure 7.** Quenching efficiency of PFE/sodium citrate and fluorescence recovery efficiency of PFE/sodium citrate/Al<sup>3+</sup> in the PBS (10 mM) with different pH values. [PFE] =  $1.0 \times 10^{-5}$  M, [sodium citrate] =  $6.0 \times 10^{-6}$  M, and [Al<sup>3+</sup>] =  $9.0 \times 10^{-6}$  M.

## CONCLUSION

In summary, a new assay method to detect Al<sup>3+</sup> ions in aqueous solution using the conjugated polyelectrolyte PFE was developed. The mechanism is based on the aggregation-sensitive fluorescence properties of PFE and the strong chelation ability of Al<sup>3+</sup>/citrate. Citrate-induced interpolymer  $\pi$ -stacking aggregation resulted in efficient self-quenching of PFE. The formation of Al<sup>3+</sup>/citrate complexes limited the quenching effect, whereas other metal ions had no effect on the fluorescence recovery of PFE. This assay has high sensitivity because of the ability of the emission of conjugated polymers to be amplified. Its simplicity and rapidity mean that this assay shows promise for the real-time detection of Al<sup>3+</sup>.

## ASSOCIATED CONTENT

### Supporting Information

UV-vis absorption spectra of PFE in DMSO/H<sub>2</sub>O with different volume ratios, fluorescence emission spectra of PFE in H<sub>2</sub>O with the successive addition of different organic salts, UV-vis absorption spectra of PFE in different concentrations of sodium citrate, quenching efficiencies of PFEMO as a

function of the concentration of organic acid salts, fluorescence emission spectra and quenching efficiencies of PFE/sodium citrate complexes in H<sub>2</sub>O in the presence of different concentrations of Al<sup>3+</sup>, and the quenching efficiency of PFE in the presence of sodium citrate and various metal ions. This material is available free of charge via the Internet at <http://pubs.acs.org>.

## AUTHOR INFORMATION

### Corresponding Author

\*E-mail: [lidong@mater.ustb.edu.cn](mailto:lidong@mater.ustb.edu.cn) (L.L.), [hefang@mater.ustb.edu.cn](mailto:hefang@mater.ustb.edu.cn) (F.H.).

### Notes

The authors declare no competing financial interest.

## ACKNOWLEDGMENTS

The authors acknowledge support from the Program for New Century Excellent Talents in Ministry of Education of China (Grant NCET-11-0576) and the Fundamental Research Funds for the Central Universities of China (Grant FRF-TP-09-006A).

## REFERENCES

- (1) Thomas, S. W.; Joly, G. D.; Swager, T. M. *Chem. Rev.* **2007**, *107*, 1339–1386.
- (2) Tang, Y.; He, F.; Yu, M.; Feng, F.; An, L.; Sun, H.; Wang, S.; Li, Y.; Zhu, D. *Macromol. Rapid Commun.* **2006**, *27*, 389–392.
- (3) Yu, M.; He, F.; Tang, Y.; Wang, S.; Li, Y.; Zhu, D. *Macromol. Rapid Commun.* **2007**, *28*, 1333–1338.
- (4) Lv, F.; Feng, X.; Tang, H.; Liu, L.; Yang, Q.; Wang, S. *Adv. Funct. Mater.* **2011**, *21*, 845–850.
- (5) Kim, I.-B.; Dunkhorst, A.; Gilbert, J.; Bunz, U. H. F. *Macromolecules* **2005**, *38*, 4560–4562.
- (6) Kim, I.-B.; Bunz, U. H. F. *J. Am. Chem. Soc.* **2006**, *128*, 2818–2819.
- (7) Lee, J.; Kim, H. J.; Kim, J. *J. Am. Chem. Soc.* **2008**, *130*, 5010–5011.
- (8) Lee, J.; Jun, H.; Kim, J. *Adv. Mater.* **2009**, *21*, 3674–3677.
- (9) Li, L.; He, F.; Wang, X.; Ma, N.; Li, L. *ACS Appl. Mater. Interfaces* **2012**, *4*, 4927–4933.
- (10) Wang, J.; Xu, X.; Shi, L.; Li, L. *ACS Appl. Mater. Interfaces* **2013**, *5*, 3392–3400.
- (11) You, J.; Kim, J.; Park, T.; Kim, B.; Kim, E. *Adv. Funct. Mater.* **2012**, *22*, 1417–1422.
- (12) Flaten, T. P. *Brain Res. Bull.* **2001**, *55*, 187–196.
- (13) Habs, H.; Simon, B.; Thiedemann, K. U.; Howe, P. *Aluminium; IPCS, Environmental Health Criteria; World Health Organization: Geneva, Switzerland, 1997; p 194.*
- (14) Delhaize, E.; Ryan, P. R. *Plant Physiol.* **1995**, *107*, 315–321.
- (15) Rout, G. R.; Samantaray, S.; Das, P. *Agronomic* **2001**, *21*, 3–21.
- (16) Arduini, M.; Felluga, F.; Mancin, F.; Rossi, P.; Tecilla, P.; Tonellato, U.; Valentinuzzi, N. *Chem. Commun.* **2003**, *13*, 1606–1607.
- (17) Quang, D. T.; Kim, J. S. *Chem. Rev.* **2010**, *110*, 6280–6301.
- (18) Kobayashi, H.; Ogawa, M.; Alford, R.; Choyke, P. L.; Urano, Y. *Chem. Rev.* **2010**, *110*, 2620–2640.
- (19) Maity, D.; Govindaraju, T. *Chem. Commun.* **2010**, *46*, 4499–4501.
- (20) Wang, L.; Qin, W.; Tang, X.; Dou, W.; Liu, W.; Teng, Q.; Yao, X. *Org. Biomol. Chem.* **2010**, *8*, 3751–3757.
- (21) Upadhyay, K. K.; Kumar, A. *Org. Biomol. Chem.* **2010**, *8*, 4892–4897.
- (22) Hau, F. K.; He, X.; Lam, W. H.; Yam, V. W. *Chem. Commun.* **2011**, *47*, 8778–8780.
- (23) Lu, Y.; Huang, S.; Liu, Y.; He, S.; Zhao, L.; Zeng, X. *Org. Lett.* **2011**, *13*, 5274–5277.
- (24) Banerjee, A.; Sahana, A.; Das, S.; Lohar, S.; Guha, S.; Sarkar, B.; Mukhopadhyay, S. K.; Mukherjee, A. K.; Das, D. *Analyst* **2012**, *137*, 2166–2175.
- (25) Sahana, A.; Banerjee, A.; Lohar, S.; Sarkar, B.; Mukhopadhyay, S. K.; Das, D. *Inorg. Chem.* **2013**, *52*, 3627–3633.
- (26) Fan, C.; Plaxco, K. W.; Heeger, A. J. *J. Am. Chem. Soc.* **2002**, *124*, 5642–5643.
- (27) Wilson, J. N.; Wang, Y.; Lavigne, J. J.; Bunz, U. H. F. *Chem. Commun.* **2003**, 1626–1627.
- (28) Ho, H. A.; Leclerc, M. *J. Am. Chem. Soc.* **2004**, *126*, 1384–1387.
- (29) Miranda, R.; You, C. C.; Phillips, R.; Kim, I.-B.; Ghosh, P. S.; Bunz, U. H. F.; Rotello, V. M. *J. Am. Chem. Soc.* **2007**, *129*, 9856–9857.
- (30) Hong, J. W.; Hemme, W. L.; Keller, G. E.; Rinke, M. T.; Bazan, G. C. *Adv. Mater.* **2006**, *18*, 878–882.
- (31) Pu, K.; Liu, B. *Macromolecules* **2008**, *41*, 6636–6640.
- (32) Li, C.; Numata, M.; Takeuchi, M.; Shinkai, S. *Angew. Chem., Int. Ed.* **2005**, *44*, 6371–6374.
- (33) Sun, H.; Feng, F.; Yu, M.; Wang, S. *Macromol. Rapid Commun.* **2007**, *28*, 1905–1911.
- (34) Satrijo, A.; Swager, T. M. *J. Am. Chem. Soc.* **2007**, *129*, 16020–16028.
- (35) He, F.; Ren, X.; Shen, X.; Xu, Q. *Macromolecules* **2011**, *44*, 5373–5380.
- (36) Shen, X.; He, F.; Wu, J.; Xu, G.; Yao, S.; Xu, Q. *Langmuir* **2011**, *27*, 1739–1744.
- (37) Cho, H. N.; Kim, D. Y.; Kim, J. K.; Kim, C. Y. *Synth. Met.* **1997**, *91*, 293–296.
- (38) Huang, Y.; Fan, Q.; Lu, X.; Fang, C.; Liu, S.; Yu-Wen, L.; Wang, L.; Huang, W. *J. Polym. Sci., Part A: Polym. Chem.* **2006**, *44*, 5778–5794.
- (39) Bunz, U. H. F. *Macromol. Rapid Commun.* **2009**, *30*, 772–805.
- (40) Chen, S.; Fang, Y.-M.; Xiao, Q.; Li, J.; Li, S.-B.; Chen, H.-J.; Sun, J.-J.; Yang, H.-H. *Analyst* **2012**, *137*, 2021–2023.
- (41) Eggins, B. R. *Chemical Sensors and Biosensors*; John Wiley & Sons, Ltd.: West Sussex, England, 2002.
- (42) Malone, S. A.; Cooper, P.; Heath, S. L. *Dalton Trans.* **2003**, 4572–4573.